HHS Public Access

Author manuscript

Nature. Author manuscript; available in PMC 2014 November 29.

Published in final edited form as:

Nature. 2014 May 29; 509(7502): 622–626. doi:10.1038/nature13251.

Piezo2 is required for Merkel cell mechanotransduction

Seung-Hyun Woo[1], **Sanjeev Ranade**[1], **Andy D. Weyer**[2], **Adrienne E. Dubin**[1], **Yoshichika Baba**[3], **Zhaozhu Qiu**[4], **Matt Petrus**[4], **Takashi Miyamoto**[1,†], **Kritika Reddy**[4], **Ellen A. Lumpkin**[3], **Cheryl L. Stucky**[2], and **Ardem Patapoutian**[1,4]

[1]Howard Hughes Medical Institute, Molecular and Cellular Neuroscience, The Scripps Research Institute, La Jolla, CA 92037, USA

[2]Department of Cell Biology, Neurobiology, and Anatomy, Medical College of Wisconsin, Milwaukee, WI 53226, USA

[3]Department of Dermatology & Physiology and Cellular Biophysics, Columbia University, New York, NY 10032, USA

[4]Genomic Institute of the Novartis Research Foundation, San Diego, CA 92121, USA

Summary

How we sense touch remains fundamentally unknown[1,2]. The Merkel cell-neurite complex is a gentle touch receptor in the skin that mediates slowly-adapting (SA) responses of Aβ sensory fibers to encode fine details of objects[3-6]. This mechanoreceptor complex was recognized to play an essential role in sensing gentle touch nearly 50 years ago[3,4]. However, whether Merkel cells or afferent fibers themselves sense mechanical force is still debated, and the molecular mechanism of mechanotransduction is unknown[1,2,7-12]. Interestingly, synapse-like junctions are observed between Merkel cells and associated afferents[6,13-15], and yet it is unclear if Merkel cells are inherently mechanosensitive or whether they can rapidly transmit such information to the neighboring nerve[1,2,16,17]. Here we show for the first time that Merkel cells produce touch-sensitive currents *in vitro*. Piezo2, a mechanically-activated (MA) cation channel, is expressed in Merkel cells. We engineered mice deficient in Piezo2 in the skin, but not in sensory neurons, and show that Merkel cell mechanosensitivity completely depends on Piezo2. In these mice, Merkel cell-neurite complex-mediated SA responses *in vivo* show reduced static firing rates, and moreover, they display moderately decreased behavioral responses to gentle touch. Our results indicate that Piezo2 is the Merkel cell mechanotransduction channel and provide the first line of

Correspondence and requests for materials should be addressed to ardem@scripps.edu..

†Current address: Gladstone Institute of Neurological Disease, San Francisco, CA 94158

Author Contributions

S.H.W. conducted experiments for Fig. 1-3 and Extended Data Fig. 1-5. A.E.D. conducted and analyzed *in vitro* electrophysiology experiments in Fig. 3 and Extended Data Fig. 5. A.D.W. performed and analyzed general skin-nerve recordings in Fig. 4a-b and Extended Data Fig. 6-7. M.P. and K.R. performed behavioral experiments in Fig. 5. S.R. generated *Piezo2*$^{fl/fl}$ mice. Z.Q. and T.M. generated *Piezo2*^{GFP} mice. During this manuscript's peer-review process, we entered into a collaboration with Y.B. and E.A.L. E.A.L. conceived, and Y.B. performed and analyzed targeted skin-nerve recordings in Fig. 4c-f. E.A.L. and C.L.S. contributed to the editing of the manuscript. S.H.W. and A.P. designed experiments and wrote the manuscript.

The authors declare no competing financial interests.

Supplementary Information is linked to the online version of the paper at www.nature.com/nature.

evidence that Piezos play a physiological role in mechanosensation in mammals. Furthermore, our data present evidence for a two-receptor site model, where both Merkel cells and innervating afferents act in concert as mechanosensors. The two-receptor system could provide this mechanoreceptor complex with a tuning mechanism to achieve highly sophisticated responses to a given mechanical stimulus[15,18,19].

We recently discovered Piezo proteins as an evolutionarily conserved mechanically-activated (MA) cation channel family[20,21]. Drosophila Piezo and zebrafish Piezo2b are shown to be involved in somatosensory mechanotransduction[22,23]. Of the two mammalian Piezo members, Piezo1 and Piezo2, Piezo2 is expressed in Dorsal Root Ganglion (DRG) sensory neurons and is required for a subset of MA currents in DRGs[20]. Here, we focused on whether Piezo2 also plays a role in somatosensory mechanotransduction in mammalian skin.

We generated a *Piezo2-GFP-IRES-Cre* knock-in reporter mouse line to detect Piezo2 expression *in vivo*. The *Piezo2-GFP-IRES-Cre* (*Piezo2*^{GFP}) allele contains Enhanced Green Fluorescent Protein (*EGFP)* fused to the C-terminal end of the *Piezo2* coding region, followed by Cre recombinase expressed through an Internal Ribosome Entry Site (IRES) (Fig. 1a). Mice carrying this allele express Piezo2-GFP fusion protein as well as Cre recombinase driven by the endogenous *Piezo2* promoter. Expression of the Piezo2-GFP fusion protein in Human Embryonic Kidney (HEK293T) cells gives rise to MA currents indistinguishable from wild type (WT) Piezo2-dependent currents (not shown). Using the *Piezo2-GFP* portion of the construct as a Piezo2 reporter, we examined Piezo2 expression in DRGs isolated from *Piezo2*^{GFP} mice as a positive control tissue[20]. When we co-stained using anti-GFP and anti-Piezo2 antibodies, GFP and Piezo2 expression patterns overlapped (Extended Data Fig. 1).

We examined both hairy and glabrous skin of *Piezo2*^{GFP} mice for Piezo2 expression. *Piezo2* was previously shown to be present at low levels in the skin by quantitative polymerase chain reaction (qPCR)[20], and here we found that GFP was specifically expressed in Merkel cells (~0.05-0.1% of total epithelial cells from dorsal skin) within whisker pad, dorsal skin, and foot pad (Fig. 1b-f, Extended Data Fig. 2a-c). We used antibodies against keratin 8 (Krt8, a marker for Merkel cells) and neurofilament heavy polypeptide (Nefh, a marker for myelinated sensory afferents) in conjunction with GFP antibody to visualize the precise localization of Piezo2 within touch domes. GFP was expressed in Merkel cells, preferentially on the side adjacent to afferent fiber innervation (Fig. 1b-f, Extended Data Fig. 2d-h). Interestingly, GFP was also present in Nefh^{+} sensory afferents, including the fibers that innervated Merkel cells (Fig. 1c, d, Extended Data Fig. 2d-h).

Due to the close proximity between Merkel cells and innervating afferents, it was difficult to convincingly conclude that GFP and Piezo2 were indeed present in Merkel cells. Therefore, we utilized *atonal homolog 1*$^{\mathrm{GFP}}$ (*Atoh1*^{GFP}) reporter mice expressing GFP in Merkel cells to purify these cells and perform qPCR analysis for *Piezo2*[24]. GFP^{+} and GFP^{-} cells from *Atoh1*^{GFP} dorsal skin were purified by fluorescence-activated cell sorting (FACS), and total RNA from these samples was subjected to qPCR for *Krt8*, *Piezo2*, and *keratin 14* (*Krt14*, a marker for basal keratinocytes and Merkel cells) (Fig. 1g, h). As expected, GFP^{+} cells

showed high expression levels of *Krt8* (Fig. 1h, *left*), suggesting they were indeed Merkel cells. Importantly, GFP^+ cells also showed high *Piezo2* levels comparable to DRG neurons, confirming *Piezo2* expression in Merkel cells (Fig. 1h, *middle*). *Piezo2* levels in GFP^- cells were minimal, consistent with our GFP immunofluoresence results in $Piezo2^{GFP}$ mouse skin as well as our previous qPCR results from skin (Fig. 1b-f)[20]. As expected, *Krt14* expression was observed in both GFP^+ and GFP^- epithelial cells, but not in DRGs. This is in agreement with GFP^- epithelial cells being mainly comprised of basal keratinocytes (Fig. 1h, *right*).

To probe the role of Piezo2 in Merkel cells, we engineered skin-specific Piezo2 knockout mice. We generated *floxed-Piezo2* mice ($Piezo2^{fl/fl}$), which contained two *loxP* sites flanking exons 43 through 45 (Fig. 2a). We targeted this specific region close to the C-terminus as it is highly conserved across different species, and moreover, the Cre excision of exons 43-45 causes a frameshift mutation in *Piezo2*, introducing an early stop codon (Extended Data Fig. 3). We crossed $Piezo2^{fl/fl}$ mice to *Krt14Cre* mice to generate $Krt14Cre;Piezo2^{fl/fl}$ conditional knockout (cKO) mice, in which Piezo2 expression is ablated in all epithelial cells including Merkel cells (Fig. 2a)[25].

$Krt14Cre;Piezo2^{fl/fl}$ cKO mice developed normally, and their skin, including Merkel cell-neurite complexes, appeared normal compared to $Piezo2^{fl/fl}$ WT littermates (Extended Data Fig. 4). To study Piezo2 deletion specifically in Merkel cells, we further generated $Krt14Cre;Piezo2^{fl/fl};Atoh1^{GFP}$ mice. This particular mouse line allowed for the purification of GFP^+ Piezo2 cKO and WT Merkel cells for qPCR (Fig. 2b, c). In GFP^+ Piezo2 cKO cells, nearly 95% of *Piezo2* transcript was degraded compared to WT, while *Piezo2* levels in DRGs from this cKO mouse were normal (Fig. 2b, c). Moreover, immunofluorescence using the Piezo2 antibody in Piezo2 cKO whisker follicles revealed that Piezo2 expression was abolished in Merkel cells (Fig. 2d, e) but still intact in afferent fibers that innervated Merkel cells (Fig. 2e, f). These results indicate that our skin-specific Piezo2 cKO mice have efficiently ablated Piezo2 only in the epithelial lineage, including Merkel cells.

Next, we addressed two important questions using Piezo2 cKO mice: are Merkel cells mechanosensitive? If yes, is this mechanosensitivity dependent on Piezo2? Using $Krt14Cre;Piezo2^{fl/fl};Atoh1^{GFP}$ and littermate controls, GFP^+ WT and Piezo2 cKO Merkel cells were FACS-purified for whole-cell patch clamp electrophysiological recordings. When Merkel cells were stimulated by gentle poking using a blunt glass probe, WT cells (n=15) responded robustly in a stimulus-dependent manner, producing rapidly adapting (RA) currents (τ=6.4 ± 1.5 msec, Fig. 3a, *left*). However, none of Piezo2-deficient Merkel cells (n=13) showed MA currents (Fig. 3a, *right*). The lack of mechanosensitivity in Piezo2-deficient cells could not be accounted for by compromised membrane properties (Extended Data Table 1).

Mechanosensitive currents were RA in voltage clamp mode. In current clamp mode, sustained depolarizations were induced by gentle mechanical stimuli in all WT but not in cKO cells (Fig. 3b, c, *top*). Subsequent voltage clamp recordings in these same cells confirmed activation of RA currents in WT cells upon mechanical stimulation (Fig. 3b, c, *middle*). Importantly, both WT and Piezo2-deficient Merkel cells were depolarized similarly by small current injections (Fig. 3b, c, *bottom*, Extended Data Table 1). We next asked

whether MA currents through Piezo2 could be responsible for the prolonged depolarization in WT cells (Fig. 3b, *top*). To answer this, we injected short duration currents with amplitudes similar to Piezo2-dependent currents, and indeed observed sustained depolarization in WT Merkel cells (Extended Data Fig. 5), suggesting that a predominant RA current could account for the observed sustained receptor potentials in these cells[26]. Other conductances may also contribute to this prolonged depolarization including voltage-gated calcium currents, which are reported to have a threshold near −20mV[17] and stochastic gating of Merkel cell membrane ion channels which could cause significant voltage fluctuations due to the high R_m of these cells (Extended Data Table 1). Thus, activation of Merkel cells by gentle touch produces a long-lasting depolarization that may ultimately contribute to the firing of SAI nerve fibers that innervate them. Collectively, these data show for the first time that Merkel cells are indeed mechanosensitive, and that Piezo2 is required in Merkel cells to produce their mechanical currents *in vitro*.

Next, we asked whether Piezo2 ablation in Merkel cells has any effect on SA responses in Aβ touch dome afferents. To answer this, we performed *ex vivo* skin-saphenous nerve recordings in *Krt14Cre;Piezo2$^{fl/fl}$* (cKO) and *Piezo2$^{fl/fl}$* (WT) littermates (Fig. 4). The overall proportions of Aβ fiber subtypes found by an electrical search stimulus were similar in both groups (Fig. 4a). Interestingly, firing frequencies of overall SA Aβ fibers at various forces were reduced in Piezo2 cKO animals compared to WT littermates, but they were not abolished (Fig. 4b). Conduction velocity of these SA fibers was also slightly reduced in cKO mice, compared to WT, but von Frey thresholds were similar in both groups (Extended Data Fig. 6). On the contrary, firing frequencies of RA Aβ fibers were comparable between cKO and WT (Extended Data Fig. 7, Extended Data Table 2).

To specifically probe the effect of Piezo2 ablation on Merkel cell-innervating SAI afferents, we used a targeted approach to record directly from touch dome afferents, which were identified by FM1-43 uptake[27]. Upon mechanical stimulation, Piezo2 cKO touch dome afferents showed noticeably short, reduced firing, compared to WT littermates (Fig. 4c, d, Extended Data Table 3). Unlike WT afferents that maintained firing for the duration of ramp-and-hold stimuli, cKO touch dome afferents produced intermediately adapting firing patterns (Fig. 4e). The number of spikes fired (Fig. 4f, Extended Data Table 3) and overall mean firing rates were significantly diminished in Piezo2 cKO touch dome afferents (17±3 Hz; n=33 displacements from 6 afferents), compared to WT (27±4 Hz; n=28 displacements from 5 afferents). This difference was more pronounced during the static stimulation phase, resulting in reduced static firing rates (Fig. 4f). Together, our data suggest that Piezo2 is required for proper mechanosensory encoding in Merkel cell-neurite complexes in the intact skin.

We next performed somatosensory behavioral assays in Piezo2 cKO and control littermates. Because Merkel cell-neurite complexes are known to mediate gentle touch sensation, we subjected these animals to tests for gentle touch, texture, and pain, which included von Frey filaments, cotton swab sensitivity of the hindpaw, texture discrimination assay, and a Randall Selitto test. For most of the above-mentioned assays, Piezo2 cKO animals behaved similarly as control littermates (not shown). Interestingly, in the automated von Frey filament test, Piezo2 cKO mice showed a significant decrease in percent paw withdrawal

response only at lower forces (1.0 g-1.5 g), but showed comparable responses to controls at higher forces (Fig. 5a). At low forces, not only were the responses less frequent, but fewer cKO mice responded (Fig. 5b). These results indicate that Piezo2 cKO mice are affected in sensing only low force mechanical stimuli, and this phenotype is in agreement with our skin-nerve recordings, which show a reduction, but not complete ablation of SA responses in Piezo2 cKO mice.

We provide answers to critical questions regarding the functionality of the Merkel cell-neurite complex. Our study is the first to show that Merkel cells display touch-sensitive currents, and that Piezo2 is required for Merkel cell mechanotransduction. This represents the first definitive evidence for a mammalian Piezo family member to be involved in mechanotransduction *in vivo*. Moreover, we show that Merkel cells play a partial role in the generation of SA responses and in gentle touch perception in mice. Interestingly, the accompanying manuscript by Maksimovic et al. demonstrates that *Krt14Cre;Atoh1*^{CKO} animals, which completely lack epidermal Merkel cells in their skin, show similar SAI firing deficits as Piezo2 cKO mice in skin-nerve recordings. This reinforces that Piezo2 is the principal Merkel cell mechanotransduction channel *in vivo*. Our current data are most consistent with a two-receptor site model, which proposes that both Merkel cells and Aβ sensory afferents are necessary for mediating proper mechanically-activated SA responses[15,18,19,28]. This model explains why SA fibers are only partially affected when Merkel cells are present but not mechanosensitive. The observed expression of Piezo2 in the afferents that innervate Merkel cells may also support this model. Analysis of the sensory afferent-specific Piezo2-deficient animal model will provide further clues to reveal the extent to which mechanotransduction is directly dependent on the nerves. Most peripheral sensory receptors are thought to have evolved with a single receptor site for sensory transduction. The Merkel cell-neurite complex is known to have the highest spatial resolution among other cutaneous mechanoreceptors, and this allows for deciphering fine spatial details such as shape, edge and curvature[5]. We speculate that mechanosensors present both at nerve endings and in Merkel cells act in concert to convey the exquisite mechanosensitivity of this complex[15,18,19].

Methods

Animals

All experimental procedures were conducted in accordance with IACUC guidelines provided by The Scripps Research Institute, Medical College of Wisconsin, and Columbia University. Animals were randomly chosen for experimental subjects, and all experimental procedures were performed in a blinded manner.

Mouse lines

Piezo2GFP-IRES-Cre (*Piezo2*^{GFP}; see below); *Atoh1*$^{GFP/GFP}$ (JAX, stock # 13593); *Piezo2*$^{fl/fl}$ (see below); *Krt14Cre* mice (JAX, stock # 4782).

Generation of Piezo2GFP-IRES-Cre (Piezo2^{GFP}) mice—An ES cell targeting construct was generated to introduce the *EGFP-IRES-Cre* sequence at the end of *Piezo2*

exon 54. A two-step cloning strategy was used to add 5' and 3' arms of homology into pL451 vector, which contains a neomycin cassette flanked by FRT sites and a unique loxP site. The 5′ arm included *Piezo2* exons 53 and 54, with a stop codon replaced by the *EGFP* coding sequence followed by an *IRES-Cre* cassette. The 5' arm was inserted into pL451, upstream of the neomycin cassette. The 3' arm contained 2.1 kb *Piezo2* genomic sequence downstream of exon 54, and was inserted into 5' arm + pL451 vector, downstream of the neomycin cassette. The entire targeting construct was sequence verified prior to ES cell electroporation. C57B6/J derived C2 ES cell clones that survived neomycin selection were screened by PCR to confirm the integration of both arms of homology. Three independent clones were chosen for blastocyst injections, and one clone led to high contribution chimeras that produced germline transmitted offspring as assayed by black coat color. This chimera line was then mated to *FLPe* mice (The Jackson Laboratory, stock # 5703) to remove the neomycin cassette and to generate heterozygous $Piezo2^{GFP}$ mice. Heterozygous $Piezo2^{GFP}$ mice were intercrossed to generate homozygous $Piezo2^{GFP}$ reporter for an enhanced GFP signal and WT littermate mice.

Generation of Piezo2 constitutive and conditional knockout mice—An ES cell targeting construct was generated that would allow for the conditional deletion of Piezo2 by the addition of loxP sites flanking exons 43-45. A three-step cloning strategy was used to add 5' and 3' arms of homology into the pL451 vector, which contains a neomycin cassette flanked by FRT sites and a unique loxP site. First, a 3.0 kb 5' arm of homology was amplified from mouse ES cell DNA and inserted into pL451, upstream of the neomycin cassette. The 3' arm of homology was then added in two sequential steps. A 2.9 kb PCR fragment was amplified that included a second loxP site in the 3' primer. This product was inserted into 5' arm + pL451, downstream of the neomycin cassette, followed by the remainder of the 3' arm. The entire targeting construct was sequence verified and linearized in preparation for ES cell electroporation. C57B6/J derived C2 ES cell clones that survived neomycin selection were screened by PCR to confirm the integration of both arms of homology. The PCR product from the 3' arm screen was gel excised and sequence verified for the integration of the second loxP site. Three independent clones were chosen for blastocyst injections, and one clone led to high contribution chimeras that produced germline transmitted offspring as assayed by black coat color. Chimeras were then mated to *EIIA-Cre* mice (The Jackson Laboratory, stock # 3724) to generate $Piezo2^{wt/-}$ mice or mated to *FLPe* mice (stock # 5703) to generate $Piezo2^{wt/fl}$ mice following the deletion of the neomycin resistance cassette. $Piezo2^{wt/-}$ mice and $Piezo2^{wt/fl}$ mice were intercrossed to generate $Piezo2^{-/-}$ and $Piezo2^{fl/fl}$ mice, respectively.

Generation of the anti-Piezo2 antibody

An mPiezo2 cDNA construct spanning amino acids 351-485 was cloned into the SpeedET vector, and the construct was expressed in bacteria to generate protein. The bacterial pellet was lysed, sonicated and purified by passing through a NiNTA resin bed. The eluate was analyzed by SDS-PAGE gel and LCMS, and further separated out by passing through a Superdex S75 column. The purified protein antigen was then supplied to Pierce antibodies, Thermofisher Scientific, Rockford, IL for injection into rabbits to generate antibodies. A two

rabbit/90 day protocol was applied to generate the polyclonal antibodies, and all final bleeds were protein G purified.

Sequence of Piezo2 protein used to generate antibodies:

LIRIWLQEPLVQEEMAKEDEGALDCSSNQNTAERRRSLWYATQYPTDERKLLSMTQ DDY
KPSDGLLVTVNGNPVDYHTIHPSLPIENGPAKTDLYTTPQYRWEPSEESSEKKEEEE DK REDSEGEGSQEEKRSVR

Antibodies

GFP (1:500, Life Technologies, A10262), Piezo2 (1:1000), Krt8 (1:1000, DSHB, TROMA-I), Nefh (1:1000, Aves lab, NFH; Abcam, ab8135), S100 (1:200, Dako, Z0311), VGLUT2 (1:100, Life Technologies, 427800), Krt14 (1:15,000, Covance, PRB-155P), and α-SMA (1:500, Sigma, C6198-2ML).

Immunofluorescence

Whisker pad, dorsal skin, footpad and DRG specimens were harvested from 3 week- or 7 week-old mice. Tissues were processed for immunostaining as previously described[30].

Fluorescent images were captured using Nikon confocal microscope C2.

Merkel cell isolation, Fluorescence-activated cell sorting (FACS), quantitative RTPCR (qPCR)

Epithelial cells including keratinocytes and Merkel cells were isolated from murine dorsal skin (P0-P5) as previously described with a few modifications[31]. Purified epithelial cells were then subjected to FACS. For subsequent qPCR analysis, cells were directly sorted into Trizol, and total RNA was isolated. For electrophysiological recordings, cells were sorted into CnT-02 media with 10% FBS. Merkel cells were cultured overnight and subjected to electrophysiological recordings the following day.

Western blotting

HEK293T cells were transfected with *pIres2-EGFP*, *mPiezo1-pcDNA3.1(-)-Ires-EGFP*, or *mPiezo2-sport6-Ires-EGFP* vectors using Lipofectamine 2000. Cells were harvested 48 hours post-transfection, and cell lysates were processed for western blotting as previously described[21].

Whole-cell electrophysiology

Whole-cell voltage clamp recordings were performed as previously described[20]. Current clamp recordings were performed as previously described[32]. Briefly, cells were continuously perfused at 23-26 °C with (in mM) 127 NaCl, 3 KCl, 1 $MgCl_2$, 2.5 $CaCl_2$, 10 dextrose, 10 HEPES (pH 7.3). Electrodes had resistances of 3.7 + 0.2 MΩ (n=25) when filled with standard CsCl based intracellular solution (in mM): 133 CsCl, 1 $CaCl_2$, 1 $MgCl_2$,

5 EGTA, 10 HEPES, 4 Mg-ATP, 0.5 Na-GTP (pH 7.3 with CsOH). Access resistance was not different between genotypes (9 ± 1 MΩ; n=19). To determine membrane potential changes in current clamp, cells were recorded using a low Clintracellular solution (in mM): 125 K-gluconate, 7 KCl, 1 $CaCl_2$, 1 $MgCl_2$, 10 HEPES, 1 tetraK-BAPTA, 4 Mg-ATP, 0.5 Na-GTP (pH 7.3 with KOH) (electrode resistances were 6 ± 1 MΩ (n=12)). The probe displacement was advanced in increments of 0.25μm.

In current clamp experiments, depolarizing current was injected in increments of 5 pA from membrane potential near −60 mV (achieved by applying hyperpolarizing bias current). Cell capacitance was determined as previously described[32]. R_m was determined using 20 mV steps at the beginning of each sweep for MA current acquisition, and membrane time constant *tau* was calculated (R_m* C_m) (Extended Data Table 1). Membrane time constant was also determined by fitting membrane depolarizations elicited by small amplitude current injections with a single exponential (Extended Data Table 1). All recordings and data analysis were performed in a blinded manner.

WT Merkel cells were very sensitive to mechanical stimulation: during advancement of the probe in 0.25 μm increments, initial responses were sometimes observed as the probe visibly touched the cell and on average were observed with 0.4 ± 0.1 μm displacement beyond the initial touch (n=15, mean ± SEM). On the other hand, Piezo2-deficient cells were not activated by 2.6 ± 0.3μm (n=13) above touching the cell (range: 1.8-4.5 μm before the recording was lost).

Skin-nerve recordings (General method for Fig. 4a, b)

Piezo2 cKO (n =12) or WT littermates (n =15) aged 7-17 weeks were sacrificed, and the hairy skin of the left and right hindpaws was shaved and dissected from the leg along with the innervating saphenous nerve. The skin-nerve preparation was then moved to a bath containing oxygenated synthetic interstitial fluid consisting of the following (in mM): 123 NaCl, 3.5 KCl, 0.7 $MgSO_4$, 1.7 NaH_2PO_4, 2.0 $CaCl_2$, 9.5 sodium gluconate, 5.5 glucose, 7.5 sucrose and 10 HEPES. The buffer was brought to a pH of 7.45 ± 0.05, and all recordings were performed with a bath temperature of 32 ± 0.5 °C. All recordings were performed with the corium side up.

The saphenous nerve was then placed on a mirror plate in a mineral oil-filled chamber and was teased apart into fine filaments and placed on a AgCl recording electrode. The majority of functionally independent fibers were identified using an electrical search stimulus, while a small number of fibers were found using a mechanical search stimulus. Figures showing percentages of fiber types were made using only those fibers found with an electrical search stimulus (Fig. 4a). After fiber isolation, the most sensitive spot of the receptive field was determined electrically, and conduction velocity was calculated. Fibers were categorized as Aβ, Aδ, or C based on their conduction velocity as previously described[33,34], with Aβ fibers conducting at velocities greater than 10m/sec, Aδ fibers between 1.2-10 m/sec, and C fibers below 1.2 m/sec. Fibers were also grouped based on the adaptation to mechanical stimuli (rapidly adapting (RA) fibers; slowly adapting (SA) fibers; mechanically insensitive (MI) fibers). Note that intermediately adapting (IA) fibers were included within the SA category

in Fig. 4a. Mechanical thresholds were obtained for each fiber type using von Frey filaments (0.044 mN (0.0045 g) to 147 mN (14.99 g)).

Recordings were digitized and displayed on an oscilloscope and recorded on a computer for analysis using a PowerLab data acquisition system and Chart 5 software. Once a functionally independent fiber was found, two-minute baseline recordings were made to determine spontaneous activity. Fibers were then subjected to a series of forces (5 mN (0.51 g), 10 mN (1.02 g), 20 mN (2.04 g), 40 mN (4.08 g), 100 mN (10.20 g), 150 mN (15.3 g), and 200 mN (20.4 g)) for 10 seconds using a feedback-controlled, computer-driven mechanical stimulator with a flat ceramic tip (diameter 1.0 mm). Action potential responses to these stimuli were recorded in LabChart, and 1-minute intervals were given between stimuli to prevent sensitization/desensitization. All recordings and data analysis were performed in a blinded manner.

Skin-nerve recordings (Directed recordings from identified touch dome afferents by FM1-43 for Fig. 4c-f)

Ex vivo skin-saphenous nerve recordings from identified touch dome afferents were performed as described (Maksimovic *et al.*, submitted). Adult female mice (7-15 week-old) were injected subcutaneously with FM1-43 (70 μl of 1.5 mM in sterile PBS) to label Merkel cells and cutaneous sensory afferents in touch domes of Piezo2 cKO and control mice. Hindlimb skin was shaved, depilated and harvested 12–14 h after injection. Skin was mounted epidermis-side-up and was continuously perfused with carbogen-buffered synthetic interstitial fluid (SIF) at 32 °C. The nerve was kept in mineral oil in a recording chamber, teased and placed onto a silver recording electrode connected with a reference electrode to differential amplifier. Ramp-and-hold displacements (0.1–1.3 mm) were delivered with a custom-built indenter probe (1.5 mm ceramic tip; 5-s hold phases). Each indentation was delivered from a point 0.6mm above the skin's surface, as indicated in Fig. 4c. One-minute intervals were given between successive stimuli. Extracellular signals were digitized and recorded using Sci-Works Experimenter software (DataWave Technologies). FM1-43-labelled Merkel cell-neurite complexes in each afferent's receptive field as visualized using a fluorescence microscope equipped with a long-pass GFP filter set. Responses from touch dome afferents were identified with a mechanical search protocol as described[4,27] (Maksimovic *et al*, submitted). Responses were classified as IA if spikes persisted through only a portion of the first 4 s of the static phase, and SA if spikes were observed throughout the duration of the 5-s hold phase. All recordings and analysis were performed blind to genotype.

Behavioral assay (von Frey filament stimulation)

Males and females aged 6-15 weeks were used in behavioral experiments. An automated von Frey apparatus (Dynamic Plantar Aesthesiometer, UGO Basile) was used to conduct experiments as described previously[35]. Mice were allowed to acclimate on a wire mesh and then were probed with von Frey filaments of defined force (g). The hind paw was probed for one second and scored for a withdrawal response. Each force was probed four times, and % withdrawal responses were calculated. The same set of withdrawal response data was also

used to calculate % responders to von Frey stimulation. Out of four stimulations, an animal that gave at least one withdrawal response was considered as a responder.

Statistics

Statistical analyses for qPCR, whole cell current density, and behavioral assays were performed using an unpaired *t* test with Welch's correction. For skin-nerve recordings, firing frequencies between WT and cKO Aβ fibers over different forces were compared using a 2-way ANOVA with Bonferroni post-hoc analysis. % of fiber types between genotypes was determined using a contingency table with Chi Square test. Analysis of conduction velocities between the two genotypes was performed using Student's *t* test, and von Frey thresholds were compared using a Mann-Whitney test. For targeted skin-nerve recordings, spike counts and mean firing rates in identified touch dome afferents (by FM1-43) were compared with Student's *t* test (two-tailed, unpaired). The proportion of IA responses between genotypes was compared using a contingency table with Fisher's exact test.

Sample size choice

For Merkel cell isolation using FACS and all immunofluorescence studies, we performed more than 10 separate experiments with different samples, and we observed consistent results from all experiments that were conducted independently. For qPCR analysis, sample sizes were chosen based on our previous studies, in which we performed at least 3 separate experiments per sample to ensure statistical significance[20]. For whole-cell electrophysiological recordings, we observed that *in vitro* recorded MA currents were either present (in all WT Merkel cells) or not (cKO). Therefore, we recorded from 15 WT Merkel cells and 13 Piezo2 cKO Merkel cells to ensure consistent results and statistical significance. For *ex vivo* skin-nerve recordings, we chose sample sizes according to the previous work of touch-sensitive afferents in $Atoh1^{CKO}$ mice[11]. Among Aβ afferents, they observed 8 SAI afferents in WT littermates (n=8/39) but none in $Atoh1^{CKO}$ genotypes (n=0/27)[11]. Therefore, we concluded that a minimum of five afferents per genotype would be sufficient to observe differences in response properties of touch dome afferents in our targeted recordings. For behavioral assays, sample sizes were chosen based on our previous studies in which we used a minimum of 8-10 animals per genotype to ensure statistical significance[35]. For all our assays, multiple cohorts were tested on multiple days so that our results were not biased. We tested 32 mice (WT littermates) and 33 mice (Piezo2 cKO) in order to ensure multiple cohorts were tested.

Acknowledgements

We would like to thank Swetha Murthy and Bertrand Coste for suggestions. Research was supported by NIH grants R01DE022358 (to A.P.) and R01AR051219 (to E.A.L.).

References

1. Abraira VE, Ginty DD. The sensory neurons of touch. Neuron. 2013; 79:618–639. [PubMed: 23972592]

2. Maksimovic S, Baba Y, Lumpkin EA. Neurotransmitters and synaptic components in the Merkel cell-neurite complex, a gentle-touch receptor. Annals of the New York Academy of Sciences. 2013; 1279:13–21. [PubMed: 23530998]

3. Chambers MR, Iggo A. Slowly-adapting cutaneous mechanoreceptors. The Journal of physiology. 1967; 192:26–27.

4. Iggo A, Muir AR. The structure and function of a slowly adapting touch corpuscle in hairy skin. The Journal of physiology. 1969; 200:763–796. [PubMed: 4974746]

5. Johnson KO. The roles and functions of cutaneous mechanoreceptors. Current opinion in neurobiology. 2001; 11:455–461. [PubMed: 11502392]

6. Halata Z, Grim M, Bauman KI. Friedrich Sigmund Merkel and his “Merkel cell”, morphology, development, and physiology: review and new results. The anatomical record. Part A, Discoveries in molecular, cellular, and evolutionary biology. 2003; 271:225–239.

7. Ikeda I, Yamashita Y, Ono T, Ogawa H. Selective phototoxic destruction of rat Merkel cells abolishes responses of slowly adapting type I mechanoreceptor units. The Journal of physiology. 1994; 479(Pt 2):247–256. [PubMed: 7799224]

8. Mills LR, Diamond J. Merkel cells are not the mechanosensory transducers in the touch dome of the rat. Journal of neurocytology. 1995; 24:117–134. [PubMed: 7745442]

9. Senok SS, Baumann KI, Halata Z. Selective phototoxic destruction of quinacrine-loaded Merkel cells is neither selective nor complete. Experimental brain research. Experimentelle Hirnforschung. Experimentation cerebrale. 1996; 110:325–334. [PubMed: 8871092]

10. Kinkelin I, Stucky CL, Koltzenburg M. Postnatal loss of Merkel cells, but not of slowly adapting mechanoreceptors in mice lacking the neurotrophin receptor p75. The European journal of neuroscience. 1999; 11:3963–3969. [PubMed: 10583485]

11. Maricich SM, et al. Merkel Cells Are Essential for Light-Touch Responses. Science. 2009; 324:1580–1582. [PubMed: 19541997]

12. Maricich SM, Morrison KM, Mathes EL, Brewer BM. Rodents rely on Merkel cells for texture discrimination tasks. The Journal of neuroscience : the official journal of the Society for Neuroscience. 2012; 32:3296–3300. [PubMed: 22399751]

13. Hartschuh W, Weihe E. Fine structural analysis of the synaptic junction of Merkel cell-axon-complexes. The Journal of investigative dermatology. 1980; 75:159–165. [PubMed: 6774030]

14. Gu J, Polak JM, Tapia FJ, Marangos PJ, Pearse AG. Neuron-specific enolase in the Merkel cells of mammalian skin. The use of specific antibody as a simple and reliable histologic marker. The American journal of pathology. 1981; 104:63–68. [PubMed: 6789681]

15. Fagan BM, Cahusac PM. Evidence for glutamate receptor mediated transmission at mechanoreceptors in the skin. Neuroreport. 2001; 12:341–347. [PubMed: 11209947]

16. Diamond J, Holmes M, Nurse CA. Are Merkel cell-neurite reciprocal synapses involved in the initiation of tactile responses in salamander skin? The Journal of physiology. 1986; 376:101–120. [PubMed: 3795072]

17. Yamashita Y, Akaike N, Wakamori M, Ikeda I, Ogawa H. Voltage-dependent currents in isolated single Merkel cells of rats. The Journal of physiology. 1992; 450:143–162. [PubMed: 1331421]

18. Cahusac PM, Mavulati SC. Non-competitive metabotropic glutamate 1 receptor antagonists block activity of slowly adapting type I mechanoreceptor units in the rat sinus hair follicle. Neuroscience. 2009; 163:933–941. [PubMed: 19596050]

19. Press D, Mutlu S, Guclu B. Evidence of fast serotonin transmission in frog slowly adapting type 1 responses. Somatosensory & motor research. 2010; 27:174–185. [PubMed: 20937000]

20. Coste B, et al. Piezo1 and Piezo2 are essential components of distinct mechanically activated cation channels. Science. 2010; 330:55–60. [PubMed: 20813920]

21. Coste B, et al. Piezo proteins are pore-forming subunits of mechanically activated channels. Nature. 2012; 483:176–181. [PubMed: 22343900]

22. Kim SE, Coste B, Chadha A, Cook B, Patapoutian A. The role of Drosophila Piezo in mechanical nociception. Nature. 2012; 483:209–212. [PubMed: 22343891]

23. Faucherre A, Nargeot J, Mangoni ME, Jopling C. piezo2b Regulates Vertebrate Light Touch Response. The Journal of neuroscience : the official journal of the Society for Neuroscience. 2013; 33:17089–17094. [PubMed: 24155313]

24. Rose MF, et al. Math1 is essential for the development of hindbrain neurons critical for perinatal breathing. Neuron. 2009; 64:341–354. [PubMed: 19914183]
25. Dassule HR, Lewis P, Bei M, Maas R, McMahon AP. Sonic hedgehog regulates growth and morphogenesis of the tooth. Development. 2000; 127:4775–4785. [PubMed: 11044393]
26. Lesniak DR, et al. Computation identifies structural features that govern neuronal firing properties in slowly adapting touch receptors. eLife. 2014; 3:e01488. [PubMed: 24448409]
27. Wellnitz SA, Lesniak DR, Gerling GJ, Lumpkin EA. The regularity of sustained firing reveals two populations of slowly adapting touch receptors in mouse hairy skin. Journal of neurophysiology. 2010; 103:3378–3388. [PubMed: 20393068]
28. Yamashita Y, Ogawa H. Slowly adapting cutaneous mechanoreceptor afferent units associated with Merkel cells in frogs and effects of direct currents. Somatosensory & motor research. 1991; 8:87–95. [PubMed: 1646558]
29. Milenkovic N, Wetzel C, Moshourab R, Lewin GR. Speed and temperature dependences of mechanotransduction in afferent fibers recorded from the mouse saphenous nerve. Journal of neurophysiology. 2008; 100:2771–2783. Additional References. [PubMed: 18815344]
30. Woo SH, Stumpfova M, Jensen UB, Lumpkin EA, Owens DM. Identification of epidermal progenitors for the Merkel cell lineage. Development. 2010; 137:3965–3971. [PubMed: 21041368]
31. Piskorowski R, Haeberle H, Panditrao MV, Lumpkin EA. Voltage-activated ion channels and Ca(2+)-induced Ca (2+) release shape Ca (2+) signaling in Merkel cells. Pflugers Archiv : European journal of physiology. 2008; 457:197–209. [PubMed: 18415122]
32. Dubin AE, et al. Inflammatory signals enhance piezo2-mediated mechanosensitive currents. Cell reports. 2012; 2:511–517. [PubMed: 22921401]
33. Koltzenburg M, Stucky CL, Lewin GR. Receptive properties of mouse sensory neurons innervating hairy skin. Journal of neurophysiology. 1997; 78:1841–1850. [PubMed: 9325353]
34. Stucky CL, et al. Overexpression of nerve growth factor in skin selectively affects the survival and functional properties of nociceptors. The Journal of neuroscience : the official journal of the Society for Neuroscience. 1999; 19:8509–8516. [PubMed: 10493751]
35. Petrus M, et al. A role of TRPA1 in mechanical hyperalgesia is revealed by pharmacological inhibition. Molecular pain. 2007; 3:40. [PubMed: 18086313]

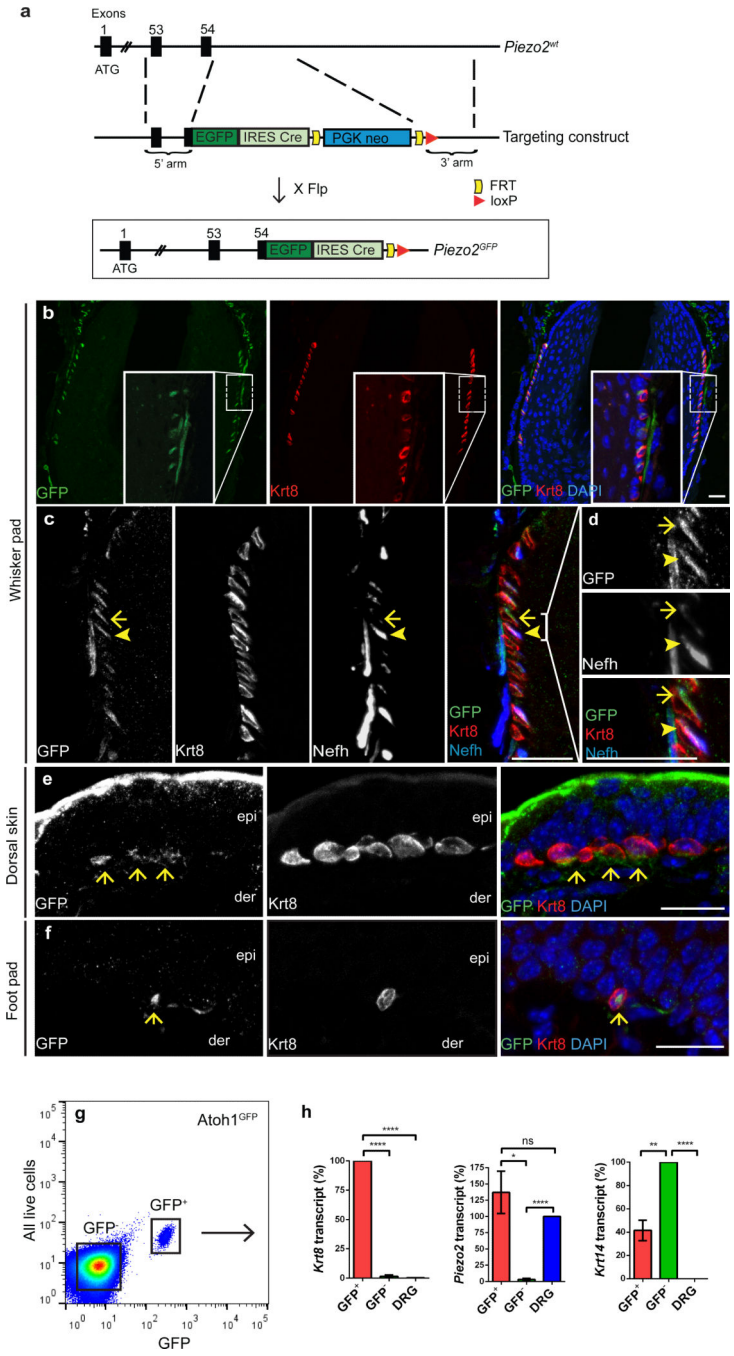

Figure 1. Piezo2 expression in hairy and glabrous skin

a, A schematic diagram of the *Piezo2*^{GFP} allele generation. Flp, flippase. **b,** GFP and Krt8 co-staining in the whisker follicle at a lower magnification. **c, d,** GFP, Krt8, and Nefh co-staining in the whisker follicle at a higher magnification. (d) shows a magnified view of the bracketed area in (c). Arrowheads mark the co-localization of GFP, Krt8, and Nefh. Note that in areas where Nefh^{+} fibers are missing, GFP and Krt8 still co-localize (arrows). **e, f,** GFP and Krt8 co-staining in a touch dome (e) and in glabrous skin (f). Arrows mark the position of Krt8^{+} Merkel cells. Scale bars b-f, 20 μm. epi, epidermis; der, dermis. **g, h,** A

representative FACS plot (out of 12 experiments) of live epithelial cells isolated from *Atoh1*^{GFP} skin (g) and qPCR analysis (n=4) of GFP^{+} and GFP^{-} cells and DRG isolated from *Atoh1*^{GFP} mouse (h). Bars represent mean ± SEM. **P* < 0.05; ***P* < 0.01; *****P* < 0.0001; ns, not significantly different, unpaired *t*-test with Welch's correction.

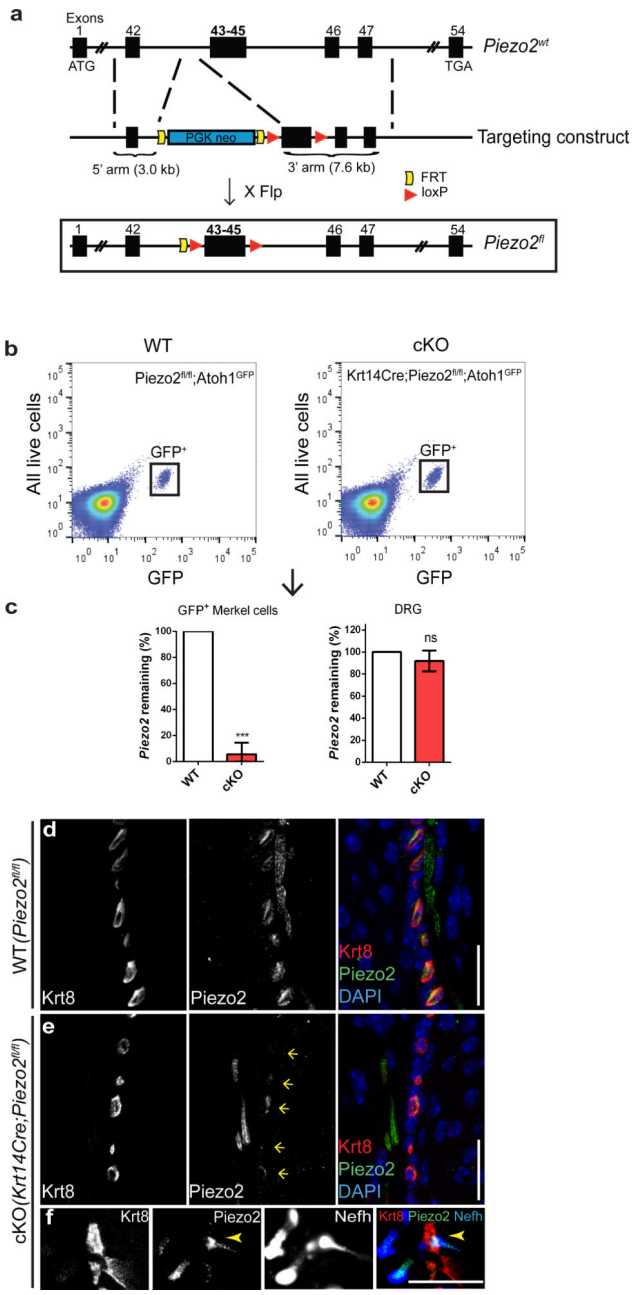

Figure 2. Generation and characterization of skin-specific *Piezo2* conditional knockout mice

a, A schematic diagram of the *Piezo2*^{fl} allele generation. Flp, flippase. **b,** Representative FACS plots (out of 9 experiments) of live epithelial cells isolated from WT and cKO dorsal skin. **c,** qPCR (n=3) analysis showing *Piezo2* levels in GFP^{+} cells and DRG of WT and cKO mice. Bars represent mean ± SEM. ***$P < 0.001$; ns, not significantly different, unpaired *t*-test with Welch's correction. **d, e,** Piezo2 and Krt8 co-staining in WT (d) and cKO (e) whisker pads. In (e), arrows mark the position of Krt8^{+} Merkel cells. **f,** Piezo2, Krt8, and Nefh co-staining in cKO whisker pad. Arrowheads mark the co-localization of Piezo2 and Nefh. Scar bars d-f, 20 μm.

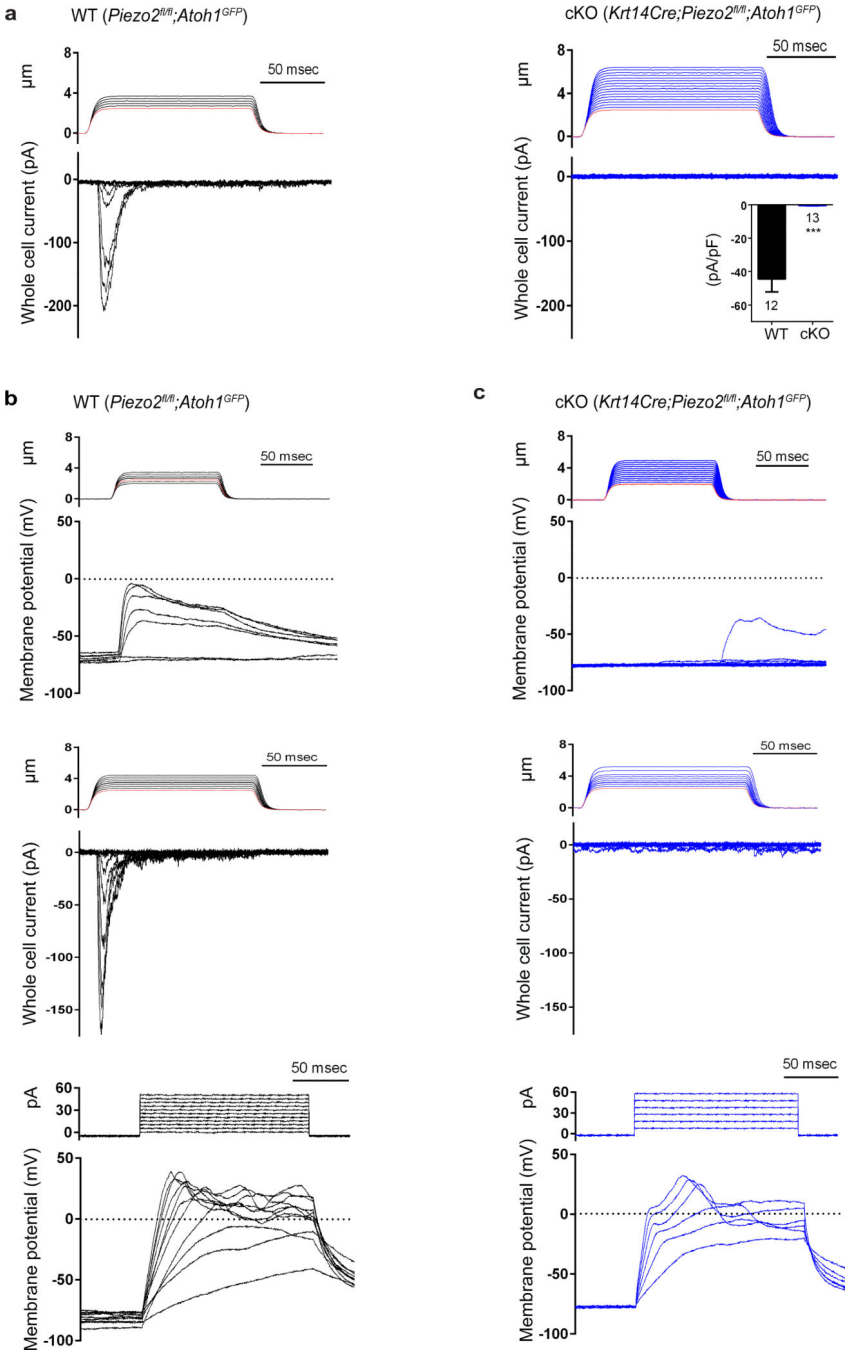

Figure 3. Mechanically activated (MA) currents in Merkel cells depend on Piezo2

a, Representative traces of MA inward currents by a gentle poking stimulus in Merkel cells from WT (*left*) and cKO (*right*). The inset shows average MA whole-cell current density measured in WT and Piezo2 cKO Merkel cells. (CsCl intracellular) Bars represent mean ± SEM. ***$P < 0.001$, Student's *t* test. **b, c,** Representative traces (out of 6 experiments) from WT (b) and Piezo2 cKO (c) Merkel cells. Current clamp recordings displaying a change in membrane potential in response to gentle mechanical stimuli (*top*); subsequent displacement assays in voltage clamp mode (*middle*); current clamp recordings showing similar changes

in membrane potential elicited by electrical stimulation (*bottom*). (K-gluconate intracellular) Red lines in stimulus traces indicate the displacement at which the probe visibly touched the cell.

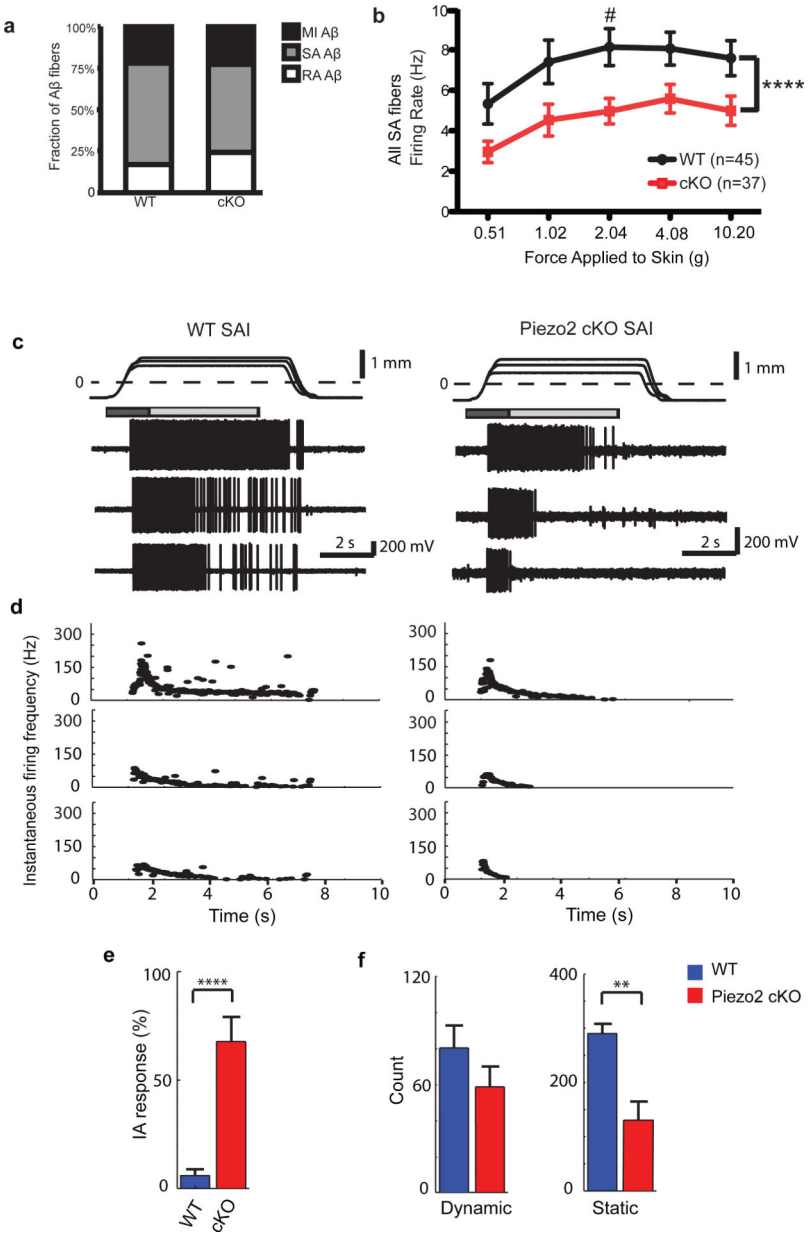

Figure 4. Ex vivo skin-saphenous nerve recordings in WT and Piezo2 cKO mice

a, Proportions of mechanically insensitive (MI), slowly adapting (SA), and rapidly adapting (RA) Aβ fibers in WT (n=59) and Piezo2 cKO mice (n=66). The relatively low RA Aβ fiber % in both groups in comparison to previous studies is likely due to the genetic background of our animals[29]. **b,** Firing rates of all SA Aβ fibers at increasing forces in WT and Piezo2 cKO. ****$P < 0.0001$; #$P < 0.05$, 2-way ANOVA with Bonferroni post-hoc analysis. **c,** Representative recordings from touch dome afferents in WT (left) vs Piezo2 cKO (right). Top traces show ramp-and-hold displacements at three magnitudes with corresponding spike trains below. Dashed line marks the point of skin contact (0 mm). Boxes indicate dynamic (dark gray: 1.5s after displacement command onset) and static phases for analysis (light gray: 4s after the beginning of hold command). **d,** Instantaneous firing frequencies of the

responses in (c). **e,** Proportion of intermediately adapting (IA) responses to supra-threshold displacements in touch dome afferents. ****P <0.0001, Fisher's exact test. **f,** Maximum number of spikes in the dynamic and static response phases. **P ≤0.01, Student's t test. Bars represent mean ± SEM. For c-f, WT n=5, Piezo2 cKO n=6 afferents. Note that for a-b, recordings were made using a force-controlled mechanical stimulator; for c-f, a displacement control was used for the directed recordings of FM1-43-labeled afferents.

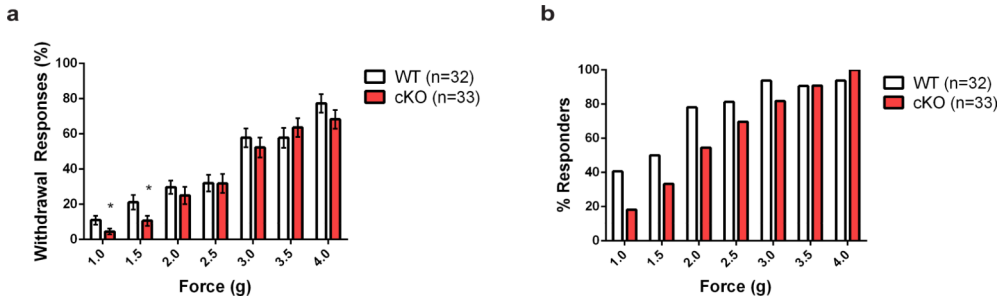

Figure 5. Gentle touch assay in WT and Piezo2 cKO mice

a, Percent paw withdrawal responses to gentle von Frey filament stimulation between 1.0 and 4.0 g forces in WT and Piezo2 cKO mice. Bars represent the mean ± SEM. **P* < 0.05, Student's *t* test. **b,** Percent mice responding to von Frey filament stimulation in WT and Piezo2 cKO.

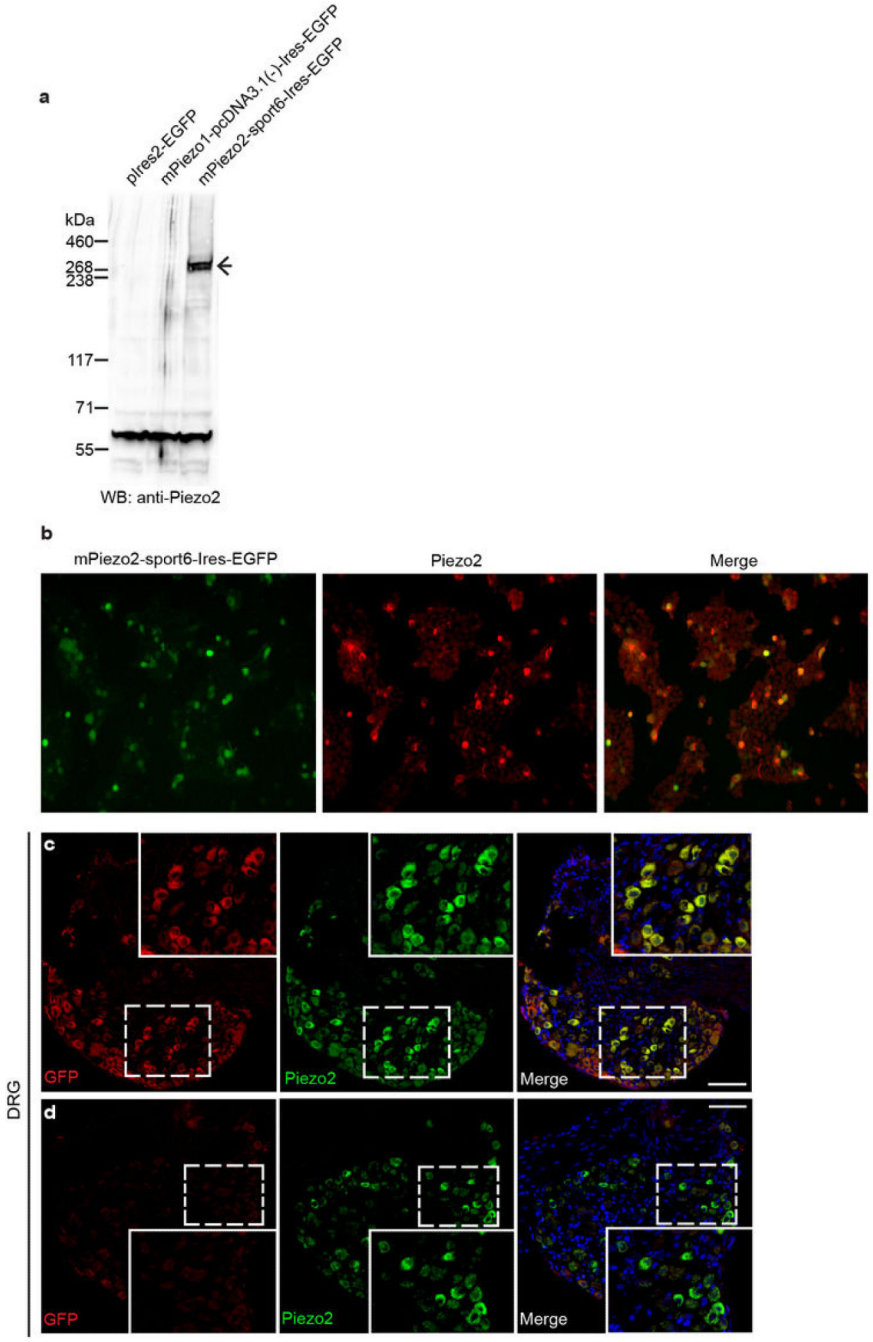

Extended Data Fig. 1. Validation of anti-Piezo2 antibody

a, Piezo2 detection by western blotting using anti-Piezo2 antibody (see full methods for antibody generation) in HEK293T cells overexpressing *pIres2-EGFP* (left lane), *mPiezo1-pcDNA3.1(−)-Ires-EGFP* (middle lane), and *mPiezo2-sport6-Ires-EGFP* (right lane). **b,** Piezo2 immunofluorescence in *mPiezo2-sport6-Ires-EGFP*-transfected HEK293T cells. The left panel shows EGFP epifluorescence in transfected cells, and the middle panel shows Piezo2 immunofluorescence in these same cells. **c, d,** Immunofluorescence of GFP and Piezo2 in adult *Piezo2*^{GFP} reporter (c) and WT littermate (d) DRG. Piezo2 expression is

observed in ~45.6 % of DRG neurons: 587 Piezo2$^{+\ \text{expressers}}$/1287 total neurons; 159 Piezo2$^{\text{high expressers}}$/587 Piezo2$^{+\ \text{expressers}}$. Scale bars c, d, 100 μm.

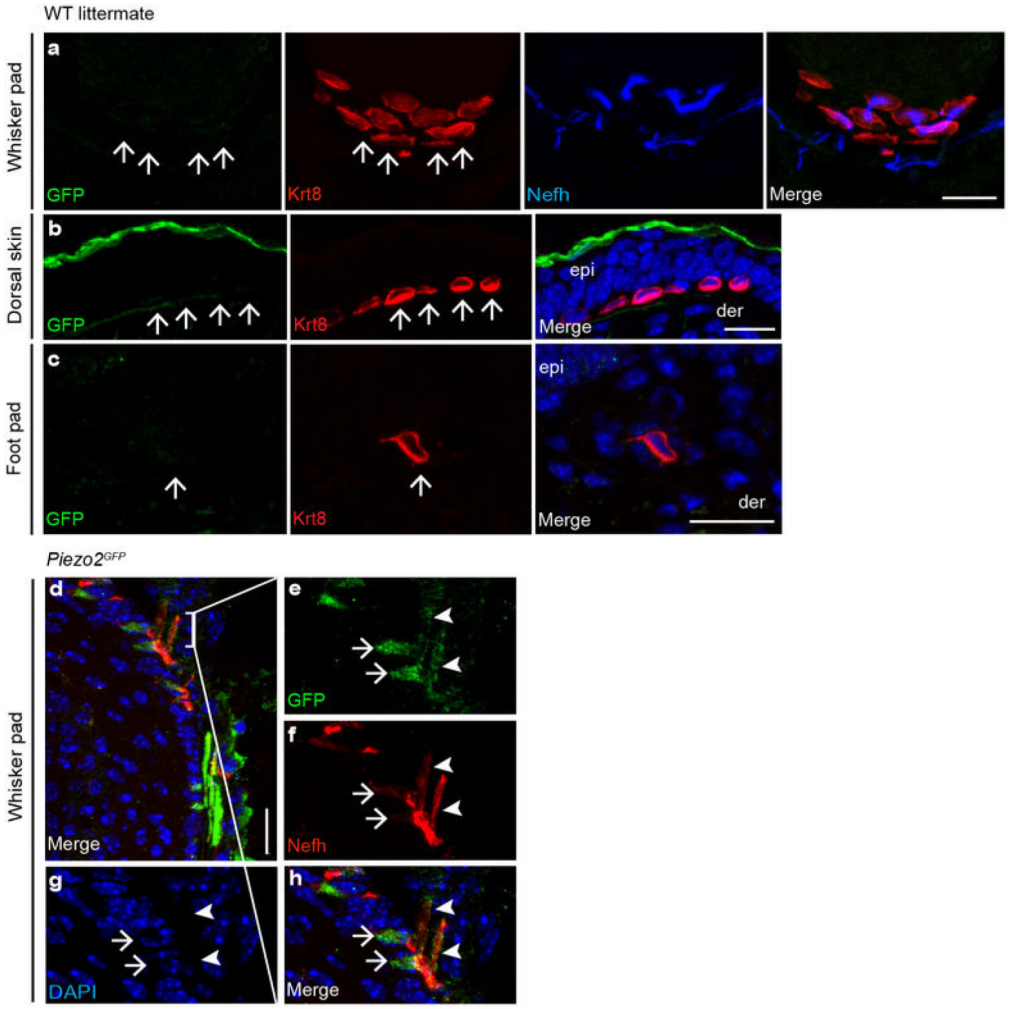

Extended Data Fig. 2. GFP immunofluorescence in WT control and *Piezo2*^{GFP} reporter mice

a, GFP, Krt8, and Nefh co-staining in WT littermate whisker follicle. **b, c,** GFP and Krt8 co-staining in WT littermate touch dome (b) and glabrous skin (c). Arrows mark the position of Krt8^{+} Merkel cells. **d-h,** GFP and Nefh co-staining in *Piezo2*^{GFP} whisker follicle. (e-h) show magnified views of the bracketed area in (d). Arrows mark GFP expression only. Closed arrowheads mark the co-localization of GFP and Nefh. Scale bars a-h, 20 μm. epi, epidermis; der, dermis.

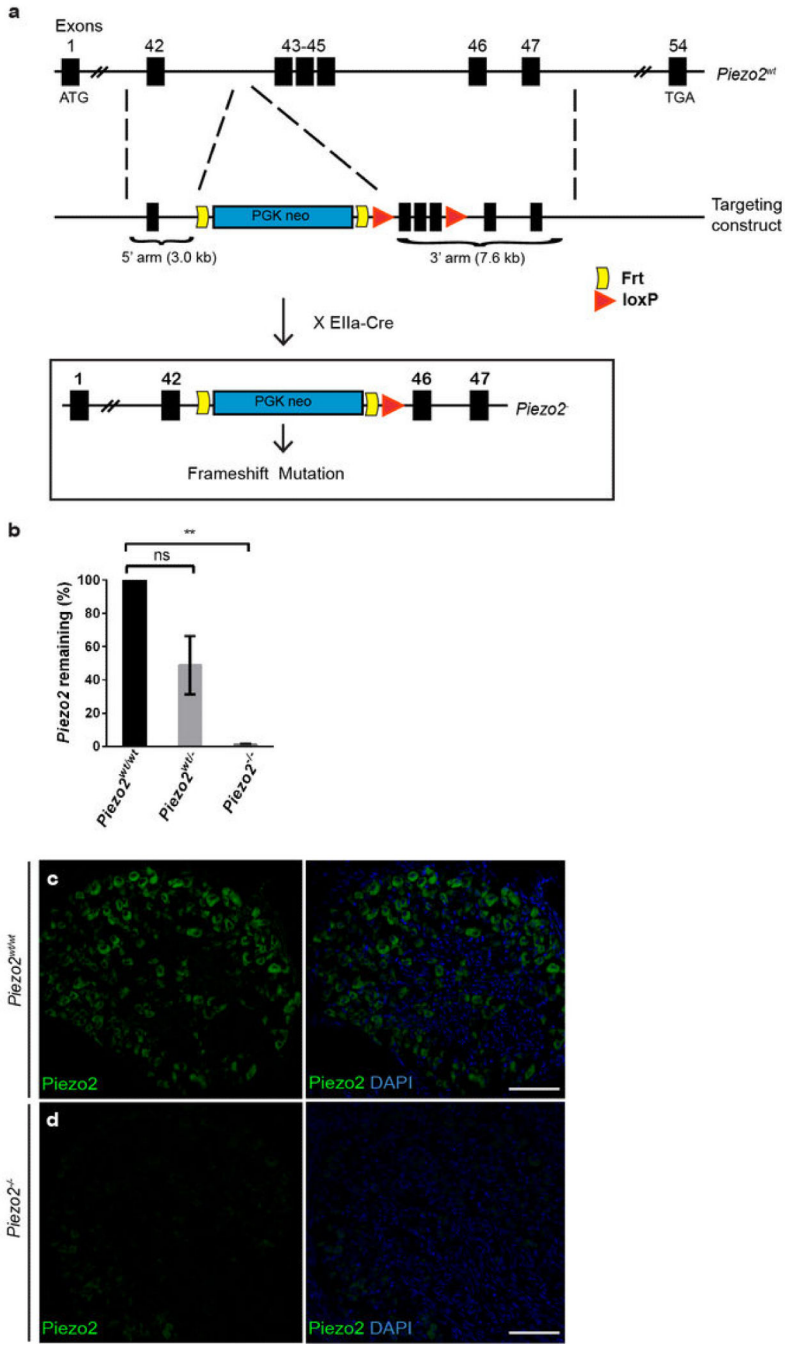

Extended Data Fig. 3. Generation of *Piezo2*-null allele (*Piezo2*$^{-}$) and characterization of Piezo2 constitutive knockout mice

a, A schematic diagram of *Piezo2*$^{-}$ allele generation. **b,** qPCR (n=2) showing *Piezo2* levels in *Piezo2*$^{wt/wt}$, *Piezo2*$^{wt/-}$, and *Piezo2*$^{-/-}$ E19.5 lungs. Error bars represent mean ± SEM. $^{**}P < 0.01$; ns, not significantly different, unpaired *t*-test with Welch's correction. **c, d,** Piezo2 immunofluorescence in WT littermate (c) and *Piezo2*$^{-/-}$ newborn DRG (d). Scale bars c, d, 100 μm.

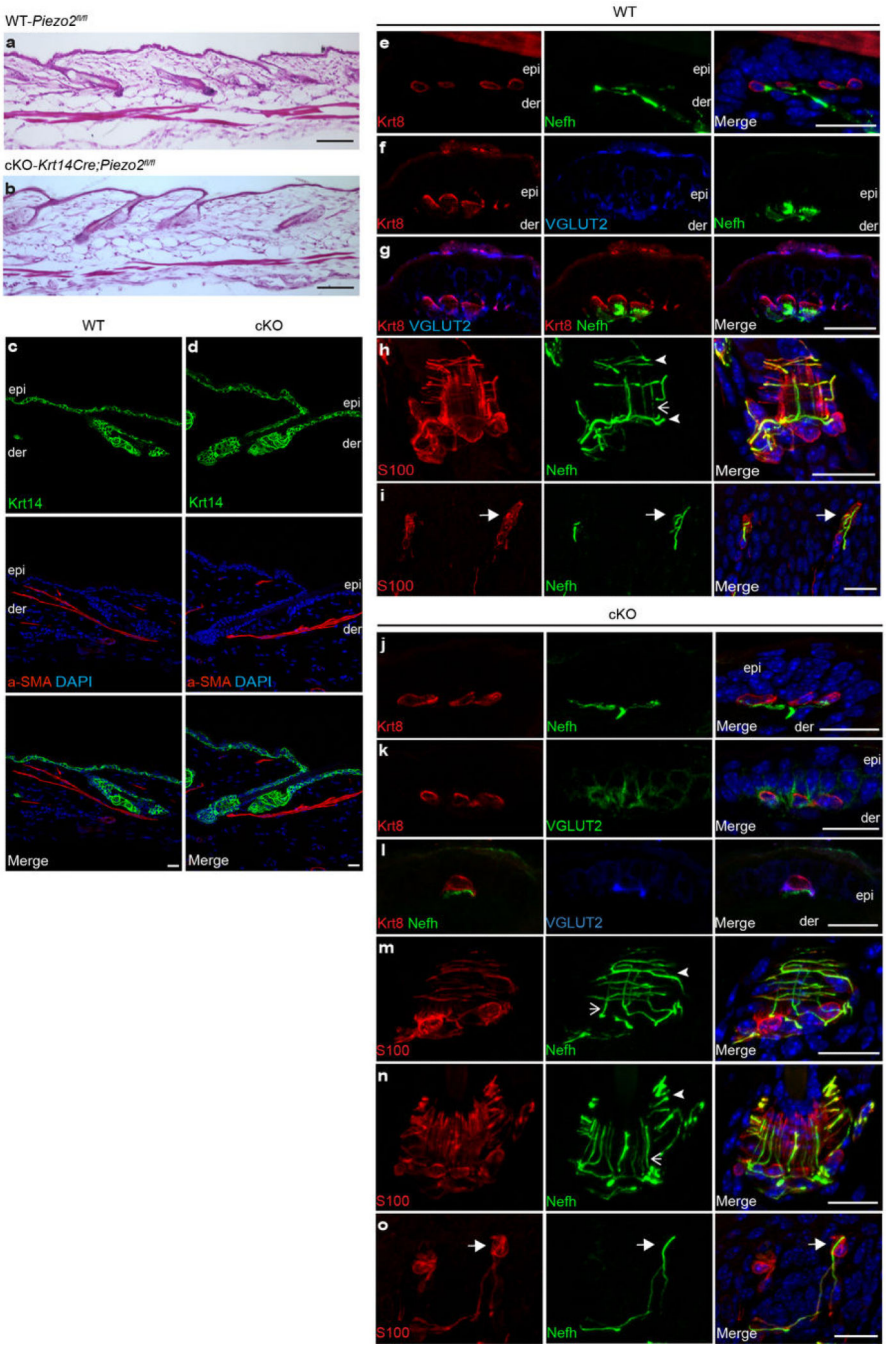

Extended Data Fig. 4. Characterization of *Piezo2*$^{fl/fl}$(WT) and *Krt14Cre;Piezo2*$^{fl/fl}$(cKO) adult skin

a, b, H&E staining of WT and Piezo2 cKO dorsal skin. **c, d,** Immunofluorescence of Krt14 and a-SMA (alpha smooth muscle actin) in WT and cKO dorsal skin. **e-g, j-l,** Epidermal touch domes co-stained with Krt8, Nefh, and VGLUT2 (vesicular glutamate transporter 2, a marker for Merkel cells) in WT and cKO dorsal skin. **h, m, n,** Lanceolate endings and circumferential fibers co-stained with S100 (S100 calcium binding protein, a marker for Schwann cells) and Nefh in WT and cKO dorsal skin. Closed arrowheads mark

circumferential fibers, and arrows mark lanceolate endings. **i, o,** Meissner's corpuscles co-stained with S100 and Nefh in WT and cKO footpads. Closed arrows mark Meissner's corpuscle. Scale bars, 100 μm (a, b), 20 μm (rest). epi, epidermis; der, dermis.

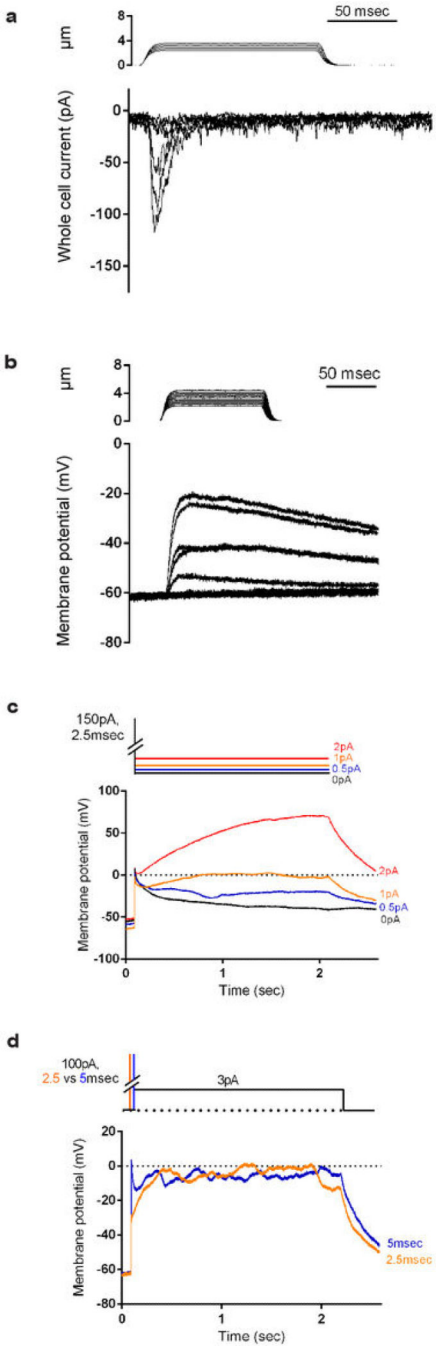

Extended Data Fig. 5. Current injections simulating Piezo2-induced currents produce prolonged depolarizations in Merkel cells *in vitro*

a, Representative traces of MA inward currents evoked by a gentle poking stimulus in a WT Merkel cell. A ramp (1 μm/msec)-and-hold displacement stimulus (0.25 μm increments) was applied to the cell in whole-cell voltage clamp configuration. The steady state current at the end of a 125 msec displacement was −6 ± 2pA (V_h= -80mV, n=15), 4% of the maximal current observed (−146 ± 29pA). **b,** Representative current clamp recordings from a WT Merkel cell, displaying a change in membrane potential in response to gentle mechanical

stimuli. **c,** Piezo2-dependent currents were simulated by injecting short current pulses followed by different levels of long lasting but small current injections. In WT Merkel cells (n=4), membrane potential changes are elicited by applying a short (2.5 msec) 150 pA current injection followed by additional current injections of 0 pA (black), +0.5 pA (blue), +1 pA (orange) and +2 pA (red) from the bias holding current (-10 pA). In the absence of any continuous current, the membrane potential slowly decays after cessation of the initial 150 pA injection, consistent with a contribution of passive membrane properties (black trace). Importantly, long lasting depolarizations are observed when these short pulses are followed by very small current injections (0.5-1 pA, which are ~10-15 % of the average observed Piezo2 current remaining at the end of the 125 msec mechanical stimulation (Fig. 3b, see above)). **d,** In WT cells (n=4), membrane potential changes are elicited by a short 100 pA current injection followed by +3 pA (half the average Piezo2-dependent MA sustained current) from the bias holding current (−10 pA). Orange line, 2.5 msec initial pulse; Blue line, 5 msec initial pulse. These data indicate that long lasting Piezo2 channel activity at levels below that observed during mechanical stimulation (panel a and Fig. 3b) is crucial for sustained membrane depolarizations in Merkel cells. The high R_m of these cells can enable small current fluctuations to produce large voltage fluctuations.

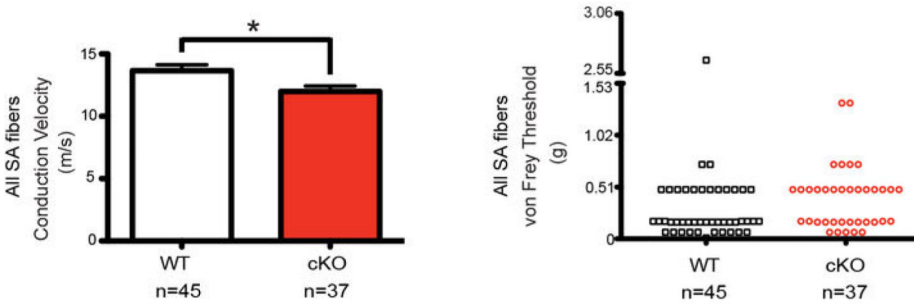

Extended Data Fig. 6. Conduction velocity and von Frey thresholds of all SA Aβ afferents in WT and Piezo2 cKO mice

Conduction velocity (*$P < 0.05$, Student's *t* test) and von Frey thresholds ($P = 0.0516$, Mann-Whitney test) of all SA Aβ fibers from WT and Piezo2 cKO mice. Error bars represent mean ± SEM.

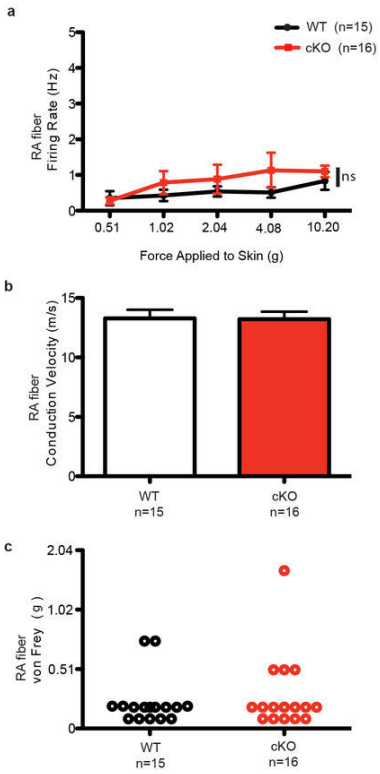

Extended Data Fig. 7. Characterization of RA Aβ afferents in WT and Piezo2 cKO mice

a, Firing rates of RA Aβ fibers in response to an increasing series of mechanical forces in WT and Piezo2 cKO mice. **b, c,** Conduction velocity (b) and von Frey thresholds (c) of RA Aβ fibers from WT and Piezo2 cKO mice.

Extended Data Table 1

Membrane properties of WT and Piezo2 cKO Merkel cells

Parameter	WT	Piezo2 cKO
Cell capacitance (pF)	2.3 ± 0.2 (n=17)	2.4 ± 0.1 (n=17)
Current at −100mV (pA)	−5 ± 1 (n=17)	−2 ± 1 (n=17)
R_m in K-gluconate (GΩ)	15 ± 2 (n=10)	14, 17 (n=2)
R_m * C_m (calculated membrane time constant) in K-gluconate (msec)	35 ± 6 (n=10)	33, 41 (n=2)
Membrane time constant determined from current clamp recordings (msec)	70 ± 17 (n=11)	60 ± 24 (n=3)
Current injection required to elicit membrane potential fluctuations (not passive change) (pA, 125 msec injection)	17 ± 5 (4)	14, 20 (n=2)
Resting potential in K-Gluconate (mV)	−22 ± 3 (n=8)	−15, −25 (n=2)

Extended Data Table 2

Afferent properties of Aβ, Aδ, and C fibers from WT and Piezo2 cKO animals.

Fiber Type	Conduction Velocity (m/s)	von Frey Threshold (mN)	n
Aβ fiber WT	13.59 ± 0.36	2.94 ± 0.47	73
cKO	13.08 ± 0.37	3.69 ± 0.43	70
Aδ fiber WT	6.41 ± 0.49	4.37 ± 1.37	22
cKO	5.08 ± 0.75	6.77 ± 1.16	16
C fiber WT	0.57 ± 0.04	3.67 ± 0.84	17
cKO	0.60 ± 0.05	5.52 ± 0.80	21

No significant differences were found in conduction velocity or von Frey threshold between the two genotypes.

Extended Data Table 3

Summary of touch dome responses for WT and Piezo2 cKO animals.

a

	Data ID	Dynamic phase				Static phase			
		Min	Max	Ave±SD	Median	Min	Max	Ave±SD	Median
Piezo2 CKO	KO 1	3.9	13.4	6.5±1.9	6.2	6.9	67.6	16.0±9.8	13.3
	KO 2	3.2	67.8	28.7±17.3	36.6	38.7	200.8	76.7±37.8	60.9
	KO 3	3.2	20.6	6.3±3.7	4.5	9.2	149.4	50.9±31.4	45.9
	KO 4	6.1	332.5	24.2±56.1	10.4	8.6	76.5	19.3±10.1	15.8
	KO 5	5.6	28.6	13.4±4.6	13	17.2	447.5	54.8±61.4	38.6
	KO 6	4.9	17.4	8.7±2.2	8.2	8.2	86.9	27.0±11.1	26.3
Control	Wild 1	5.1	23.5	9.6±4.0	8.1	4.1	50.6	14.7±5.0	14.9
	Wild 2	9.1	295.3	22.2±48.2	11.0	4.8	54.0	16.7±7.2	14.6
	Wild 3	2.5	51.1	5.4±5.4	3.4	3.0	190.3	12.4±16.8	6.1
	Wild 4	3.3	23.3	6.2±3.5	4.9	3.9	40.2	11.8±5.3	10.3
	Wild 5	4.1	245.7	10.2±26.9	6.1	6.4	42.8	14.2±5.7	13.1

b

	Data ID	Ratio of IR(%)	Num. of SP. in Dynamic	Num. of SP. in Static	CoV
Piezo2 CKO	KO 1	0.42	79	250	0.61
	KO 2	1	25	29	0.49
	KO 3	1	95	78	0.62
	KO 4	0.14	35	207	0.52
	KO 5	0.89	58	70	1.12
	KO 6	0.60	57	147	0.41
Control	Wild 1	0	61	271	0.34
	Wild 2	0	45	239	0.43
	Wild 3	0.13	110	321	1.35
	Wild 4	0.10	102	338	0.45
	Wild 5	0.07	81	282	0.40

a, Summary of inter-spike intervals (ISIs) for touch-evoked responses. For each afferent, the maximal response was selected as representative data for further analysis. Dynamic phase: period from stimulus onset (when the indenter began moving) to end of ramp phase (when the indenter reached the hold displacement depth). Static phase: initial 4s period after indenter reached commanded displacement. Unit

of all values were milliseconds. Min: minimum. Max: maximum. Ave: average. SD: standard deviation. **b**, Summary of touch dome responses. IR: intermediate response. Num of SP: number of spikes. CoV: coefficient of variation of ISIs in the static phase.